

# Journal of Materials Chemistry A

Accepted Manuscript



This is an *Accepted Manuscript*, which has been through the Royal Society of Chemistry peer review process and has been accepted for publication.

*Accepted Manuscripts* are published online shortly after acceptance, before technical editing, formatting and proof reading. Using this free service, authors can make their results available to the community, in citable form, before we publish the edited article. We will replace this *Accepted Manuscript* with the edited and formatted *Advance Article* as soon as it is available.

You can find more information about *Accepted Manuscripts* in the [Information for Authors](#).

Please note that technical editing may introduce minor changes to the text and/or graphics, which may alter content. The journal's standard [Terms & Conditions](#) and the [Ethical guidelines](#) still apply. In no event shall the Royal Society of Chemistry be held responsible for any errors or omissions in this *Accepted Manuscript* or any consequences arising from the use of any information it contains.

# Directly Coat TiO<sub>2</sub> on Hydrophobic NaYF<sub>4</sub>:Yb,Tm Nanoplates and Regulate Their Photocatalytic Activities with the Core Size

Cite this: DOI: 10.1039/x0xx00000x

Received 00th January 2012,  
Accepted 00th January 2012

DOI: 10.1039/x0xx00000x

www.rsc.org/

Wankui Su,<sup>ab</sup> Mengmeng Zheng,<sup>a</sup> Lei Li,<sup>b</sup> Kun Wang,<sup>b</sup> Ru Qiao,<sup>\*a</sup> Yijun Zhong,<sup>a</sup> Yong Hu,<sup>a</sup> and Zhengquan Li<sup>\*ab</sup>

We demonstrate a facile method to directly coat a TiO<sub>2</sub> layer on hydrophobic NaYF<sub>4</sub>:Yb,Tm upconversion nanocrystals. Through modifying the hydrophobic nanocrystals with a surfactant layer, a conventional sol-gel route can be applied on them for TiO<sub>2</sub> deposition. The prepared β-NaYF<sub>4</sub>:Yb,Tm@TiO<sub>2</sub> show obvious photocatalytic activity under near-infrared light as well as ultraviolet light. Based on the success in preparing upconversion cores with different sizes and subsequent TiO<sub>2</sub> coating, we have systematically investigated the effect of core sizes on their photocatalytic performance. The results suggest that upconversion fluorescence of the core and surface are of the shell both have great effect on their photocatalytic activities. A moderate core size is thus preferred due to the competition of these two effects.

## 1. Introduction

Solar energy has been widely regarded as one of the promising renewable energy in the world due to its unique advantages such as natural, free, non-polluting and inexhaustible.<sup>1-4</sup> Photocatalysts with capability of utilizing solar energy have been constantly recognized as one kind of prospective materials for applications in controlling pollutant and producing new energy.<sup>5-8</sup> Among various photocatalysts, undoubtedly, titanium dioxide (TiO<sub>2</sub>) is the most widely used one for its high stability, low-cost and non-toxicity and high efficiency.<sup>9-12</sup> However, a big limitation of TiO<sub>2</sub> is its wide band gap which requires to be activated under ultraviolet (UV) or higher energy light that only occupies *ca.* 5% in the solar spectrum, much lower than visible light (48%) or near-infrared (NIR) light (43%).<sup>13-14</sup> To extend light utilization of TiO<sub>2</sub> to visible region, much effort has been devoted in recent years and a few useful approaches have been developed such as metal or nonmetal doping, deposition of noble metals, and coupling with other semiconductors.<sup>15-20</sup> Nevertheless, there is still less attention has been paid to the development of NIR-driven TiO<sub>2</sub> photocatalysts aiming to improve light utilization of solar energy in the NIR region.

Combination of upconversion (UC) materials with TiO<sub>2</sub> provides a good solution to increase the utilization of NIR light for TiO<sub>2</sub> photocatalysts and enhance their photocatalytic activities in the solar spectrum. Through upconverting two or more NIR photons to be a UV photon, the UC materials can serve as a light transducer to provide extra UV light for TiO<sub>2</sub> upon NIR irradiation. Recently, several attempts have been made to the synthesis of composite materials consisting of a

TiO<sub>2</sub> shell and a UC core such as lanthanide-doped YF<sub>3</sub>, CaF<sub>2</sub> LaF<sub>3</sub> and NaYF<sub>4</sub>.<sup>21-30</sup> Among these composites, hexagonal-phase (β-) NaYF<sub>4</sub> has been proven to be the best core material due to its higher UC efficiency than others.<sup>26-29</sup> While in most reported β-NaYF<sub>4</sub>@TiO<sub>2</sub> particles, the core particles were usually microscale rods which are generally prepared by hydrothermal method and as such the whole NaYF<sub>4</sub>@TiO<sub>2</sub> particles were much big in size,<sup>26-29</sup> limiting their potential applications (e.g., in biology) and showing low surface area for photocatalysis. Qin tried the synthesis of small NaYF<sub>4</sub>@TiO<sub>2</sub> nanoparticles (NPs),<sup>30</sup> however, the core nanocrystals (NCs) were cubic-phase (α-) NaYF<sub>4</sub> which had lower UC efficiency than the β-phase one. For deposition of TiO<sub>2</sub> shell on hydrophobic NCs, an SiO<sub>2</sub> interlayer was inevitably employed for surface-modification of NCs,<sup>26</sup> while an extra interlayer inevitably reduced energy transfer from the UC core to the TiO<sub>2</sub> shell. Direct coating TiO<sub>2</sub> on small β-NaYF<sub>4</sub> NCs should be an optimal choice to achieve the best photocatalytic performance.

To realize the synthesis of small β-NaYF<sub>4</sub>@TiO<sub>2</sub> NPs, challenges generally come from two aspects: 1) high-quality β-NaYF<sub>4</sub> NCs are generally prepared in high-temperature non-hydrolysis environment and these NCs possess a hydrophobic surface;<sup>31-34</sup> 2) conventional sol-gel process for TiO<sub>2</sub> coating cannot be directly applied on hydrophobic NCs since they cannot be well disperse in polar solvents. To address above issues, here we present a facile surfactant-mediate method to directly coat a TiO<sub>2</sub> layer on hydrophobic β-NaYF<sub>4</sub> NCs in this work. The role of surfactant not only transfers the hydrophobic NCs to be hydrophilic ones but also provides a good surface for

TiO<sub>2</sub> deposition *via* the conventional sol-gel process. Since the layer of surfactant is much thin and can be facilely removed in post-treatment, there is no any barrier between the NaYF<sub>4</sub> core and TiO<sub>2</sub> shell, greatly facilitating the energy transfer between two materials.

This facile coating method also built a highway for the combination of TiO<sub>2</sub> and various β-NaYF<sub>4</sub> NCs since uniform and size-/shape-controllable NaYF<sub>4</sub> NCs can be reproducibly obtained in the non-hydrolysis condition.<sup>31-34</sup> In previous developed UCNCs@TiO<sub>2</sub> particles, little attention has been paid in the systematic investigation of their photocatalytic activities associated with the size and shape of core NCs, although the effect of TiO<sub>2</sub> shell has been frequently explored. Based on our success in preparation of β-NaYF<sub>4</sub> NCs with different sizes, in this work we also systematically investigate the photocatalytic activity of β-NaYF<sub>4</sub>@TiO<sub>2</sub> NPs in association with their core sizes. Our work clearly suggests that both parameters, the intensity of UC fluorescence and surface area of TiO<sub>2</sub>, both play an important role in determining their final activities. As a result of the competition of these two effects, β-NaYF<sub>4</sub>@TiO<sub>2</sub> NPs with a moderate UC cores show the best photocatalytic performance. This work may shed us some new lights on the design and synthesis of composite photocatalysts consisting of UC cores and semiconductor shells.

## 2. Experimental

### 2.1 Synthesis and modification of NaYF<sub>4</sub>:Yb,Tm nanoplates

High-quality NaYF<sub>4</sub>:25%Yb,0.3%Tm nanoplates were synthesized using a user-friendly method we previously developed.<sup>31</sup> The prepared nanoplates were dispersed in a certain amount of cyclohexane, reaching a concentration of 0.1 M. To modify the particle surface, a reverse micelle method was employed.<sup>35-36</sup> In a typical process, 0.05 g cetyltrimethyl ammonium bromide (CTAB) and 1 mL of nanoplates solution were added in 20 mL DI water under vigorous stirring in a flask. Once a milky solution was formed, the flask was put in a water-bath (set at 80 °C) to slowly evaporate cyclohexane. After the milky solution gradually became transparent, the solution was removed from the water-bath and cooled down to room-temperature. The CTAB modified nanoplates (NaYF<sub>4</sub>:Yb,Tm/CTAB) were then collected from the solution by centrifuging at a speed of 8 000 rpm. After washed with water twice, the products were finally dispersed in 10 mL isopropanol.

### 2.2 Synthesis of NaYF<sub>4</sub>:Yb,Tm@TiO<sub>2</sub> NPs

Core-shell NaYF<sub>4</sub>:Yb,Tm@TiO<sub>2</sub> NPs were synthesized by directly coating a TiO<sub>2</sub> layer on the surface of NaYF<sub>4</sub>:Yb,Tm/CTAB NPs. In a typical synthesis, 10 mL of NaYF<sub>4</sub>:Yb,Tm/CTAB NPs solution (in isopropanol), 2.5 mL water and 0.3 mL ammonia (28 wt. %) were mixed in a 25-mL flask under magnetic stirring. Subsequently, 10 mL of titanium diisopropoxide bis(acetylacetonate) (TDAA) solution (10 mM, in isopropanol) was slowly injected to the solution. The mixed

solution was then aged in the flask under magnetic stirring for 12 h at room-temperature (20 °C). Core-shell NaYF<sub>4</sub>:Yb,Tm@A-TiO<sub>2</sub> (amorphous TiO<sub>2</sub>) NPs were then collected by centrifuge at a speed of 6 000 rpm from the solution. After washed with ethanol and isopropanol twice, the products were dried in vacuum for 4 h. To achieve crystalline anatase TiO<sub>2</sub> shell, the products was annealed at 500 °C for 3 h in an oven under an air atmosphere.

### 2.3 Characterizations

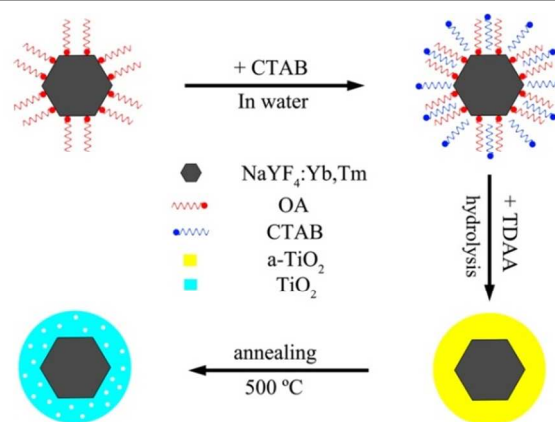
Powder X-ray diffraction (XRD) was carried out on a Philips X' Pert Pro X-ray diffractometer equipped with a Cu Kα radiation. Transmission electron microscopy (TEM) was performed on a JEOL 2010F TEM. The TEM samples were prepared by dropping a suspension of NPs on a carbon-film coated copper grid. Fluorescence spectra were acquired on a Hitachi F-7000 spectrometer equipped with a commercial 980 nm NIR laser. UV-Vis absorption spectra were obtained on a Shimadzu UV-2450 UV-Vis spectrometer.

### 2.4 Photocatalytic measurements

Photocatalytic activities of NaYF<sub>4</sub>:Yb,Tm@TiO<sub>2</sub> NPs were evaluated by degradation of RhB solution under irradiation of a Xe lamp (set at 50 W). Different irradiation bands were obtained through rationally choosing following filters: UV band-pass (300–400 nm), visible band-pass (400–780 nm) and NIR band-pass (780–2500 nm). In a typical process, 7 mg of as-prepared products was put into 50 mL of RhB solution (5 × 10<sup>-5</sup> M) in a beaker. The solution was then stirred for 12 h in dark to reach an adsorption–desorption equilibrium between the NPs and the solution. Subsequently, the beaker was exposed to the irradiation of Xe lamp accompanying with suitable filters for 30 min. Aliquots were intermittently collected at given time intervals to measure the concentration of RhB by UV-vis spectroscopy.

## 3. Results and discussion

### 3.1 Synthetic strategy



**Scheme 1** Schematic illustration of the synthetic procedure for preparation of NaYF<sub>4</sub>:Yb,Tm@TiO<sub>2</sub> core-shell NPs. (a-TiO<sub>2</sub>: amorphous TiO<sub>2</sub>)

The synthetic process from hydrophobic  $\text{NaYF}_4:\text{Yb,Tm}$  nanoplates to crystalline  $\text{NaYF}_4:\text{Yb,Tm}@\text{TiO}_2$  NPs are illustrated in Scheme 1. The  $\text{NaYF}_4:\text{Yb,Tm}$  nanoplates were prepared using oleic acid (OA) as a ligand, exhibiting uniform sizes and regular shapes. However, these nanoplates possess a hydrophobic surface which hinders applying conventional sol-gel process to coat a  $\text{TiO}_2$  layer on them, due to the requirement of polar solvents. To modify the hydrophobic surface of nanoplates to be hydrophilic, a layer of CTAB molecules is proposed to be attached around these nanoplates through *van de Walls* interaction, leaving their hydrophilic heads pointing outward. This step can be realized by reverse-micelle method using cyclohexane (i.e., nanoplates solution), CTAB and water to serve as oil-phase, surfactant and aqueous-phase, respectively (see Scheme S1). In a reverse-micelle, surfactant CTAB molecules are driven to be covered on the nanoplates when the cyclohexane solution was gradually evaporated. After surface-modification with CTAB molecules, these nanoplates will display water-dispersibility and can be well-dispersed in many polar solvent. Specifically, these nanoplates can be dispersed in a mixed solvent of isopropanol, water and ammonia, which facilitates the deposition of  $\text{TiO}_2$  via a typical sol-gel process. Upon the addition of TDAA, a slow hydrolysis titanium precursor,<sup>37-38</sup> an amorphous  $\text{TiO}_2$  layer was then deposited on these nanoplates. Crystalline  $\text{TiO}_2$  shell (anatase phase) was sequentially obtained through annealing the samples in air. Compared with previous syntheses, this CTAB-mediated route can produce high quality  $\text{NaYF}_4:\text{Yb,Tm}@\text{TiO}_2$  NPs with small particle sizes, high surface area, facilitated energy transfer and high UC fluorescence from cores.

### 3.2 Morphology and phase of samples

TEM images of samples at different stages verify above synthetic process. Fig. 1A shows the morphology of the prepared  $\text{NaYF}_4:\text{Yb,Tm}$  nanoplates. These nanoplates have a side length of 25 nm (diameter of 50 nm). Because of the hydrophobic tails from surface-attached OA molecules, a few nanoplates are self-assembled together using their lateral planes on the TEM grid. After surface modification with a CTAB layer, these nanoplates are readily dispersed in water. No obvious change in size or uniformity after modification is found on TEM measurement due to the much thin layer of CTAB molecules (Fig. 1B). Once a sol-gel process for  $\text{TiO}_2$  deposition is finished, an evident shell about 10 nm appears on these nanoplates (Fig. 1C and inset). Nanoporous pores are created in the shell after annealing the sample in air, while the core nanoplates remain unchanged (Fig. 1D). Different lattice fringes can be observed on the core and on the shell, corresponding to (100) plane of  $\beta$ - $\text{NaYF}_4$  crystal and (101) plane of anatase  $\text{TiO}_2$  crystal, respectively (inset of Fig. 1D). Note that the thin layer of CTAB molecules is removed during the annealing process. As such, the  $\text{TiO}_2$  shell and the  $\text{NaYF}_4:\text{Yb,Tm}$  core are closely contacted in the final core-shell NPs.

Fig. 2A gives XRD patterns of the  $\text{NaYF}_4:\text{Yb,Tm}$  nanoplates before and after  $\text{TiO}_2$  coating. Diffraction peaks from the

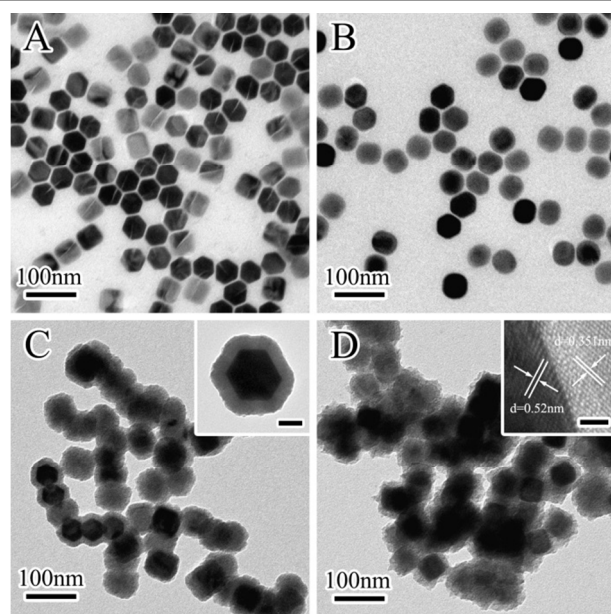


**Fig. 1** TEM images of  $\text{NaYF}_4:\text{Yb,Tm}$  nanoplates at different synthetic stages: (A) primitive NC; (B) CTAB-modified; (C) covered with an amorphous  $\text{TiO}_2$  shell; (D) after annealing. Insets are magnified TEM images of corresponding samples (Scale bars are 10 nm and 2 nm in C and D, respectively).

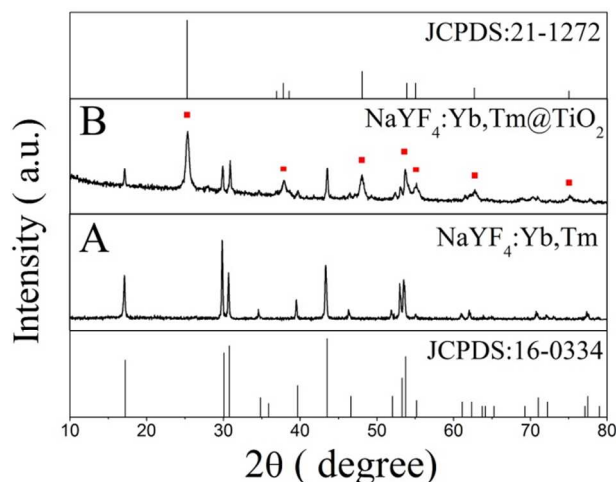


**Fig. 2** XRD patterns of (A) primitive  $\text{NaYF}_4:\text{Yb,Tm}$  nanoplates and (B)  $\text{NaYF}_4:\text{Yb,Tm}@\text{TiO}_2$  NPs after annealing. Standard patterns of  $\text{NaYF}_4$  and  $\text{TiO}_2$  crystals are given for references. Peaks from  $\text{TiO}_2$  crystal in the sample are marked in red.

nano-plates can be clearly indexed to  $\beta$ -phase  $\text{NaYF}_4$  crystals (JCPDS no. 16-0334). No peaks from cubic-phase crystals or impurities are found, suggesting high purity and crystallinity of the sample. Once the  $\text{TiO}_2$  shell was deposited on the nanoplates and annealed in air, two sets of diffraction peaks appear in the XRD patterns. One set of peaks are consistent with the  $\beta$ -phase  $\text{NaYF}_4$  crystals, while the other set of peaks matches well with anatase  $\text{TiO}_2$  crystals (JCPDS no. 21-1272). This result further confirms that a crystalline  $\text{TiO}_2$  shell have been created on the  $\text{NaYF}_4:\text{Yb,Tm}$  nanoplates.

### 3.3 UC spectra and photocatalytic mechanism

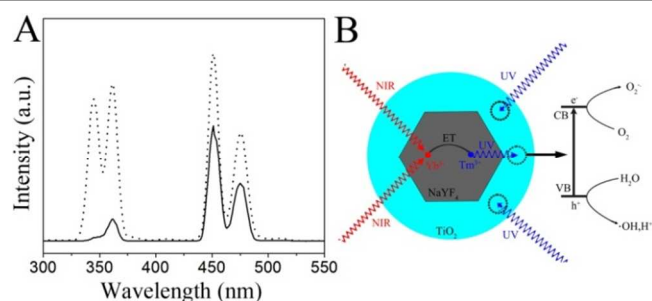


**Fig. 3** (A) UC spectra of primitive NaYF<sub>4</sub>:Yb,Tm nanoplates (dash) and annealed NaYF<sub>4</sub>:Yb,Tm@TiO<sub>2</sub> NPs (solid); (B) Schematic illustration of working mechanism of NaYF<sub>4</sub>:Yb,Tm@TiO<sub>2</sub> NPs under irradiation of UV and NIR lights. (ET: energy transfer)

UC photoluminescent spectra of the NaYF<sub>4</sub>:Yb,Tm nanoplates were shown in Fig. 3A. Upon NIR excitation, two strong peaks appear in the UV region centered at 347 nm and 362 nm. These emissions can be assigned to the transitions of <sup>1</sup>I<sub>6</sub>-<sup>3</sup>F<sub>4</sub> and <sup>1</sup>D<sub>2</sub>-<sup>3</sup>H<sub>6</sub> of Tm<sup>3+</sup> ions, respectively.<sup>39-41</sup> Besides the UV emissions, two visible emissions at 452 nm and 476 nm are also exhibited, resulting from the <sup>1</sup>D<sub>2</sub>-<sup>3</sup>F<sub>4</sub> and <sup>1</sup>G<sub>4</sub>-<sup>3</sup>H<sub>6</sub> transitions of Tm<sup>3+</sup> ions.<sup>42-43</sup> After being coated with a TiO<sub>2</sub> shell, one can find that the UV emissions from the core-shell NPs decreased evidently, while peak intensities of the visible emissions only reduced slightly. Particularly, intensity ratio of UV-to-Vis emissions has been greatly reduced, suggesting that most UV emissions have been absorbed by the coated TiO<sub>2</sub> shell. In contrast, the visible emissions only reduced a little due to light-scattering of the TiO<sub>2</sub> shell.

Photocatalytic mechanism of the prepared NaYF<sub>4</sub>:Yb,Tm@TiO<sub>2</sub> is shown in Fig. 3B. Under the UV light, the TiO<sub>2</sub> shell can directly produce electron-hole pairs and generate ROS species in solution to activate photocatalytic reactions. When these NPs are exposed under NIR light, the core NaYF<sub>4</sub>:Yb,Tm can serve as a light transducer to emit UV light through a typical upconverting process. These UV emissions from core nanoplates can be directly absorbed by the surface TiO<sub>2</sub> shell. As such, the TiO<sub>2</sub> shell can also produce ROS species even under the NIR light. Obviously, the prepared NaYF<sub>4</sub>:Yb,Tm@TiO<sub>2</sub> NPs can be activated under either UV or NIR, or both.

### 3.4 Photocatalytic activities of samples

Photocatalytic activities of the prepared NaYF<sub>4</sub>:Yb,Tm@TiO<sub>2</sub> NPs have been evaluated under different irradiation bands of a Xe lamp, using the degradation of RhB dye as a model. Under the UV band (300-400 nm), the concentration of RhB solution decrease very fast with a small amount of NPs, showing good catalytic activity of the TiO<sub>2</sub> shell deposited on the nanoplates (Fig. 4A). When the same catalytic reactions are carried out under the NIR band (780-2500 nm), a notable decrease in RhB concentration is also observed within 30 min (Fig. 4B), although decrease rate is not comparable to that under the UV band. This result implies that the NaYF<sub>4</sub>:Yb,Tm@TiO<sub>2</sub> can also work under pure NIR band, confirming that these core-shell NPs can serve as NIR-driven

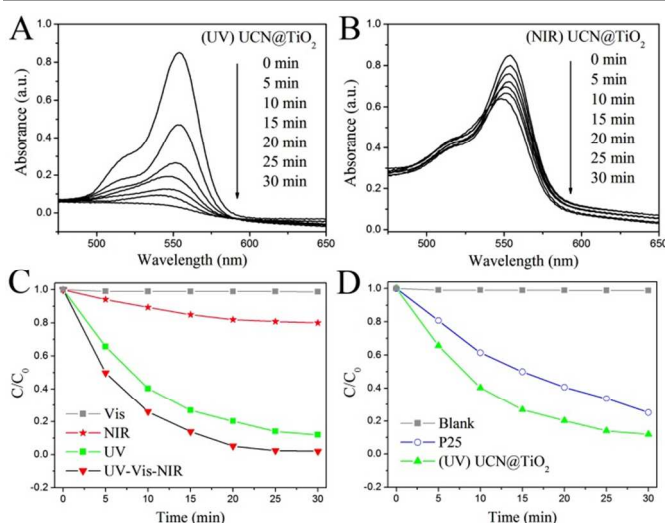


**Fig. 4** UV-Vis absorption of RhB solution catalysed by NaYF<sub>4</sub>:Yb,Tm@TiO<sub>2</sub> NPs under different irradiation bands of a Xe lamp: (A) UV band; (B) NIR band; (C) and (D) are comparisons of samples under different irradiation bands. (UCNs: NaYF<sub>4</sub>:Yb,Tm)

photocatalysts. Control experiment is also carried out in the visible band (400-780 nm), while no obvious decrease in RhB concentration is found (Fig. 4C). At the same time, fast degradation of RhB solution within 30 min can be realized under the full spectrum of Xe lamp (300-2500 nm), suggesting improved catalytic activity of NPs due to synergetic effect of both UV and NIR lights. Commercial P25 powder was also employed to verify the high activity of prepared samples. It is found that our NPs show better performance than P25 even only under the UV band, based on the same amount of TiO<sub>2</sub> content (Fig. 4D). This result is attributed to the core-shell configuration of NPs since a larger surface area is expected on core-shell NPs than that on solid powders. At the same time, high-temperature annealing would produce many nanoporous holes on the TiO<sub>2</sub> shell which also enlarge the effective surface of NaYF<sub>4</sub>:Yb,Tm@TiO<sub>2</sub> NPs.

### 3.5 Effect of core sizes

NaYF<sub>4</sub>:Yb,Tm nanoplates with different sizes were also prepared by varying the reaction time and concentration of ligands, and these nanoplates can also be facily coated with a TiO<sub>2</sub> shell *via* the similar process. For instance, NaYF<sub>4</sub>:Yb,Tm nanoplates of 100 nm and 130 nm were prepared, respectively, and TEM images of them before and after TiO<sub>2</sub> coating are shown in Fig. 5. With the increase in particle size, hexagonal front shape of nanoplates become more evident and monodispersity of particles after TiO<sub>2</sub> coating get improved. We also tried the synthesis of 30 nm NaYF<sub>4</sub>:Yb,Tm nanoplates, however, many agglomerates are found in the final sample after TiO<sub>2</sub> coating and annealing (see Fig. S1).

Size controllable NaYF<sub>4</sub>:Yb,Tm nanoplates offer us a chance to study the photocatalytic activities of NaYF<sub>4</sub>:Yb,Tm@TiO<sub>2</sub> NPs in relation with their core sizes. For comparison, the photocatalytic activities of four NaYF<sub>4</sub>:Yb,Tm@TiO<sub>2</sub> NPs with 30 nm, 50 nm, 100 nm and 130 nm cores (termed as NP30,

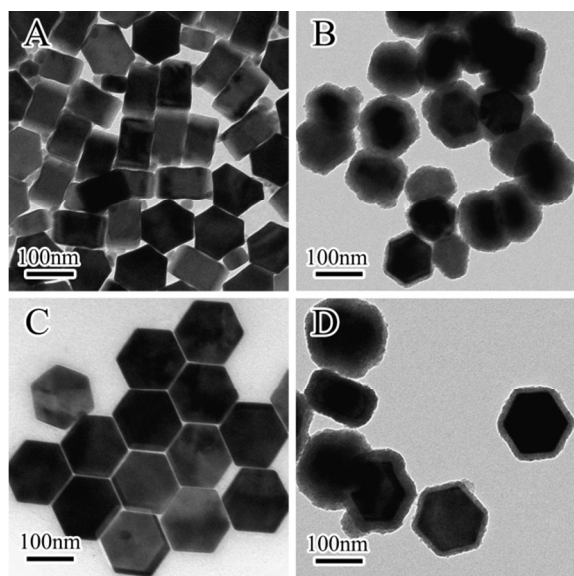


Fig. 5 TEM images of NaYF<sub>4</sub>:Yb,Tm nanoplates of different sizes before and after TiO<sub>2</sub> coating. (A) and (B) are of 100 nm nanoplates; (C) and (D) are of 130 nm nanoplates.

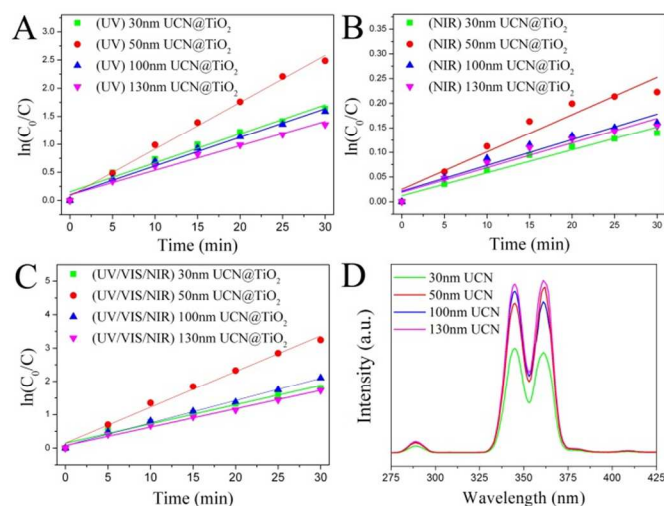


Fig. 6 Apparent rate constants of NaYF<sub>4</sub>:Yb,Tm@TiO<sub>2</sub> NPs with different core sizes under varied irradiation bands: (A) UV band; (B) NIR band; (C) UV-Vis-NIR band. (D) A comparison of UV emissions from primitive NaYF<sub>4</sub>:Yb,Tm nanoplates with different sizes before TiO<sub>2</sub> coating.

NP50, NP100 and NP130) have been investigated, respectively, and the results are shown in Fig. 5. Since photocatalytic degradation of RhB follows pseudo first-order kinetics, we express the catalytic efficiencies of different samples with apparent rate constant ( $k = \ln(C_0/C)/t$ ) (see Tab. S1). Under the UV band, NP50 sample shows significantly stronger catalytic efficiency than NP100 and NP130 (Fig. 5A). This result suggests that small UC core is beneficial to the photocatalytic performance of TiO<sub>2</sub> shell, since more surface area can be realized on small nanoplates due to the increase in particle number. However, NP30 which were expected to show the high efficiency, only gives comparable efficiency to NP100 under the UV band, lower than NP50. This result may be resulted

from their agglomerate morphology which may reduce their effective surface area to some extent (see Fig. S1).

Upon NIR irradiation, NP50 still shows the highest efficiency while NP30 exhibits the lowest efficiency among these four samples (Fig. 5B). To investigate the effect of UC fluorescence on the photocatalytic efficiencies of final samples, we have also measured the UV emissions of four primitive NaYF<sub>4</sub>:Yb,Tm nanoplates (Fig. 5D). The 30 nm UCNs display a relatively weak UC fluorescence compared with other three samples, because of more surface defects on small NCs. Once the size is above 50 nm, however, the particle size only has slightly effect on their total UC fluorescence, due to the improved crystallinity of NCs. This result is consistent with previous reports.<sup>44</sup> Combining two parameters together, the core UC intensities and surface TiO<sub>2</sub> activities under the UV band (Fig. 5A), one can easily understand that the NP50 can give the best efficiency than the other samples. For small NP30, the shell only has a moderate UV-activated efficiency and the core has a relatively lower UC fluorescence. As a result, it is reasonable that this sample just gives the lowest efficiency in the NIR band.

#### 4. Conclusions

In summary, we have demonstrated a facile route to synthesize core-shell NaYF<sub>4</sub>:Yb,Tm@TiO<sub>2</sub> NPs. Conventional sol-gel process for TiO<sub>2</sub> deposition can be directly applied on hydrophobic NCs after modification with a surfactant layer. The prepared core-shell NPs have been well characterized by TEM, XRD and PL, and their photocatalytic activities have been evaluated under different irradiation bands. As expected, these core-shell NPs can work under both UV and NIR bands, and show excellent activities due to their high surface area and strong UC fluorescence. Core-shell NPs with different core sizes are also prepared and the effect of UCNs sizes on their photocatalytic activities has been discussed. In addition to photocatalysis, these NaYF<sub>4</sub>:Yb,Tm@TiO<sub>2</sub> NPs may also offer other promising applications, such as in dye-sensitized solar cells, water splitting and photodynamic therapy.

#### Acknowledgements

The authors acknowledge financial support from National Nature Science Foundation of China (nos 21273203 and 21201151).

#### Notes and references

- <sup>a</sup> Institute of Physical Chemistry, Zhejiang Normal University, Jinhua, Zhejiang 321004, P. R. China.  
<sup>b</sup> Department of Materials Physics, Zhejiang Normal University, Jinhua, Zhejiang 321004, P. R. China.  
 Electronic Supplementary Information (ESI) available: synthesis of nanoplates, TEM images of 30 nm nanoplates and apparent rate constants of samples. See DOI: 10.1039/b000000x/

- 1 G. Michael, *Acc. Chem. Res.* 2009, **42**, 1788.

- 2 A. Shane and M. Gerald, *Chem. Soc. Rev.*, 2009, **38**, 115.
- 3 A. Hagfeldt, G. Boschloo, L. Sun, L. Kloo and H. Pettersson, *Chem. Rev.*, 2010, **110**, 6595.
- 4 M. Zhou, X. W. Lou and Y. Xie, *Nano Today*, 2013, **8**, 598.
- 5 M. R. Hoffmann, S. T. Martin, W. Choi and D. W. Bahnemann, *Chem. Rev.*, 1995, **95**, 69.
- 6 K. Akihiko and M. Yugo, *Chem. Soc. Rev.*, 2009, **38**, 253.
- 7 M. N. Chong, B. Jin, C. W. K. Chow and C. Saint, *Water Res.*, 2010, **44**, 2997.
- 8 H. Tong, S. X. Ouyang, Y. P. Bi, N. Umezawa, M. Oshikiri and J. H. Ye, *Adv. Mater.*, 2012, **24**, 229.
- 9 X. B. Chen and S. S. Mao, *Chem. Rev.*, 2007, **107**, 2891.
- 10 F. Han, V. S. R. Kambala, M. Srinivasan, D. Rajarathnam and R. Naidu, *Appl. Catal. A-Gen.*, 2009, **359**, 25.
- 11 G. Liu, L. Z. Wang, H. G. Yang, H. M. Cheng and G. Q. Lu, *J. Mater. Chem.*, 2010, **20**, 831.
- 12 J. S. Chen, C. P. Chen, J. Liu, R. Xu, S. Z. Qiao and X. W. Lou, *Chem. Commun.*, 2011, **47**, 2631.
- 13 M. D. Hernandez-Alonso, F. Fresno, S. Suarez and J. M. Coronado, *Energy Environ. Sci.*, 2009, **2**, 1231.
- 14 C. C. Chen, W. H. Ma and J. C. Zhao, *Chem. Soc. Rev.*, 2010, **39**, 4206.
- 15 R. Asahi, T. Morikawa, T. Ohwaki, K. Aoki and Y. Taga, *Science*, 2001, **293**, 269.
- 16 S. Sakthivel and H. Kisch, *Angew. Chem., Int. Ed.*, 2003, **42**, 4908.
- 17 I. Lee, J. B. Joo, Y. Yin and F. Zaera, *Angew. Chem., Int. Ed.*, 2011, **50**, 10208.
- 18 R. Long, K. Mao, M. Gong, S. Zhou, J. Hu, M. Zhi, Y. You, S. Bai, J. Jiang, Q. Zhang, X. Wu and Y. J. Xiong, *Angew. Chem. Int. Ed.*, 2014, **53**, 3205.
- 19 X. B. Cao, Z. F. Lu, L. W. Zhu, L. Yang, L. Gu, L. L. Cai and J. Chen, *Nanoscale*, 2014, **6**, 1434.
- 20 C. Z. Wen, Q. H. Hu, Y. N. Guo, X. Q. Gong, S. Z. Qiao and H. G. Yang, *Chem. Commun.*, 2011, **47**, 6138.
- 21 W. Qin, D. Zhang, D. Zhao, L. Wang and K. Zheng, *Chem. Commun.*, 2010, **46**, 2304.
- 22 L. Ren, X. Qi, Y. Liu, Z. Huang, X. Wei, J. Li, L. Yang and J. Zhong, *J. Mater. Chem.*, 2012, **22**, 11765.
- 23 Z. Li, C. Li, Y. Mei, L. Wang, G. Du and Y. Xiong, *Nanoscale*, 2013, **5**, 3030.
- 24 G. B. Shan and G. P. Demopoulos, *Adv. Mater.*, 2010, **22**, 4373.
- 25 S. Huang, L. Gu, C. Miao, Z. Lou, N. Zhu, H. Yuan and A. Shan, *J. Mater. Chem. A*, 2013, **1**, 7874.
- 26 L. Liang, Y. Liu, C. Bu, K. Guo, W. Sun, N. Huang, T. Peng, B. Sebo, M. Pan, W. Liu, S. Guo and X. Z. Zhao, *Adv. Mater.*, 2013, **25**, 2174.
- 27 Y. Zhang and Z. Hong, *Nanoscale*, 2013, **5**, 8930.
- 28 D. X. Xu, Z. W. Lian, M. L. Fu, B. Yuan, J. W. Shi and H. J. Cui, *Appl. Catal., B*, 2013, **142-143**, 377.
- 29 W. Wang, M. Ding, C. Lu, Y. Ni and Z. Xu, *Appl. Catal., B*, 2014, **144**, 379.
- 30 Y. Tang, W. Di, X. Zhai, R. Yang and W. Qin, *ACS Catal.*, 2013, **3**, 405.
- 31 Z. Li, Y. Zhang and S. Jiang, *Adv. Mater.*, 2008, **20**, 4765.
- 32 F. Wang and X. Liu, *Chem. Soc. Rev.*, 2009, **38**, 976.
- 33 C. Li and J. Lin, *J. Mater. Chem.*, 2010, **20**, 6831.
- 34 M. Haase and H. Schafer, *Angew. Chem., Int. Ed.*, 2011, **50**, 5808.
- 35 Z. Hou, C. Li, P. Ma, G. Li, Z. Cheng, C. Peng, D. Yang, P. Yang and J. Lin, *Adv. Funct. Mater.*, 2011, **21**, 2356.
- 36 Q. Tao, Z. Li and Y. Zeng, *J. Mater. Res.*, 2012, **27**, 2101.
- 37 W. Su, T. Zhang, L. Li, J. Xing, M. He, Y. Zhong and Z. Li, *RSC Adv.*, 2014, **4**, 8901.
- 38 Z. She, S. Liu, S. Zhang, K. Shah, M. Han, *Chem. Commun.*, 2011, **47**, 6689.
- 39 C. Li, Z. Quan, J. Yang, P. Yang and J. Lin, *Inorg. Chem.*, 2007, **46**, 6329.
- 40 A. Xia, Y. Gao, J. Zhou, C. Y. Li, T. S. Yang, D. M. Wu, L. M. Wu, F. Y. Li, *Biomater.*, 2011, **32**, 7200.
- 41 A. Yin, Y. Zhang, L. Sun and C. Yan, *Nanoscale*, 2010, **2**, 953.
- 42 M. K. G. Jayakumar, N. M. Idris and Y. Zhang, *PNAS*, 2012, **109**, 8483.
- 43 F. Shi and Y. Zhao, *J. Mater. Chem. C*, 2014, **2**, 2198.
- 44 H. X. Mai, Y. W. Zhang, L. D. Sun and C. H. Yan, *J. Phys. Chem. C*, 2007, **111**, 13721.